Low-Latency Analog Processors for Performance Control of MEMS

Y. Han, Z. Zhu, A. Abrol, J. V. Clark

Electrical and Computer Engineering
Mechanical Engineering
Auburn University, Auburn, AL, USA

ABSTRACT

Towards faster feedback response for controlling the performance of microelectromechanical systems (MEMS), we present the first use of the mathematical processing properties of bipolar junction transistors (BJT) for such control. This concerns a type of feedback control called performance-on-demand MEMS (PODMEMS), where the movement of the proof mass is monitored, and a feedback force is applied that is proportional to its displacement, velocity, and acceleration, which increases or decreases the system's effective stiffness, damping, or mass. A low-latency feedback response is necessary for stability. In our prior work we proposed the use of opamp-based electronics, which yielded a latency of 50 nanoseconds, which is adequate for systems that operate at hundreds of kHz or less. But for systems that operate at higher rates, lower latency is desired. In this paper we show how the latency can be reduced by an order of magnitude by using the mathematical properties of BJTs.

Keywords: performance on demand, low-latency feedback, BJT, PODMEMS

1 INTRODUCTION

Problems with the performance of microelectron-mechanical systems (MEMS) include: process variations that prevent any two MEMS from performing identically; geometric limitations of micromachining that limit the range of possible values for stiffness, damping, and mass; and post-process variations caused by thermal drift, aging, and packaging stresses.

For low-latency signal processing of feedback for controlling the response behavior of MEMS, we explore the use of analog processing circuits based on bipolar junction transistors (BJTs). By monitoring the state of the proof mass of a MEMS device, and feeding back a force onto the proof mass that is proportional to (or a function of) the state, then the apparent mass, damping, and stiffness of the MEMS device can be significantly altered [1]. To maximize stability, it is necessary that the sensed state be processed and fed back in the smallest amount of time. Typically, tens of nanoseconds are a low enough latency for MEMS that operate on a time-scale of tens to hundreds of kilohertz. A larger domain of stability allows a MEMS device to achieve a larger range of values for apparent mass, damping, and stiffness. Our prior work studied the effect of using analog feedback circuit comprised of filters and operational amplifiers, which resulted in latency of fifty nanoseconds [1]. The latency of the present work is at least five times smaller, which increases the stability domain by over a magnitude.

We model the MEMS and BJT-based feedback electronics as an equivalent circuit, which we simulate using a circuit solver. Due to high input impedance, small nonlinear distortion, and high-temperature stability of those circuits, extremely small currents from the state sensors of the MEMS can be detected and shaped. Meanwhile, the feedback circuit presented in this study has a high operating speed and a small delay, which will improve the stability of the whole device by a great amount and greatly extend the dynamic performance range. Circuit components of our BJT-based processing components, such as multiplication, square rooting, integration, and differentiation [2] will be combined to perform the necessary mathematical operations on the feed through signal of the MEMS device to achieve the desired response behavior.

2 POD TECHNOLOGY

In this section, we first describe how PODMEMS works and factors that influence the system's stability. We then introduce our new BJT-based feedback circuit and the equivalent circuit used to represent the MEMS structure.

2.1 Performance Control

Performance control is achieved by monitoring the state of MEMS proof mass and feeding back a processed signal back onto the proof mass that is a function of the instantaneous state (Figure 1, testcase).

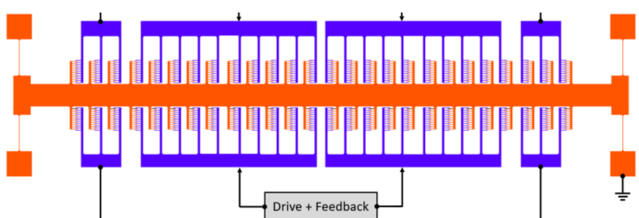

Figure 1: MEMS + feedback diagram for our PODMEMS testcase.

The mechanical equation of motion is

$$\begin{aligned} M\ddot{x}+D\dot{x}+Kx &= F_{dr}-F_{fb}(x_\tau,\dot{x}_\tau,\ddot{x}_\tau) \\ &= F_{dr}-[F_K+F_D+F_M] \\ &= F_{dr}-[K_e x_\tau + D_e\dot{x}_\tau + M_e\ddot{x}_\tau] \end{aligned} \quad (1)$$

where M, D, and K are the mass, damping, and stiffness of the mechanical system, F_{dr} is the driving force, { x, $\dot{x}$, $\ddot{x}$ } is the state of the proof mass, and F_{fb} is the feedback force that is a function of the state. The feedback force is sum of state forces $F_K = K_e x_\tau$, $F_D = D_e\dot{x}_\tau$, $F_M = M_e\ddot{x}_\tau$, which that are proportional to delayed sensed displacement x_τ, velocity $\dot{x}_\tau$, and acceleration $\ddot{x}_\tau$. A slight delay τ in the processing circuit causes the feedback response to be based on what the state used to be few nanoseconds ago; i.e., $x_\tau = x(t-\tau)$. The feedback proportionalities K_e, D_e, and M_e are the electrically-generated stiffness, damping, and mass that contribute to the overall behavior of the proof mass. They can be positive or negative. It is necessary for τ to be much smaller than the time constant of the mechanical system. In essence, if τ is small enough, (1) can be approximated as $M_{eff}\ddot{x}+D_{eff}\dot{x}+K_{eff}x=F_{dr}$, where $M_{eff}=M+M_e$, $D_{eff}=D+D_e$, and $K_{eff}=K+K_e$.

The size of the delay τ affects the domain of stability of the PODMEMS system. From an eigenvalue analysis of the characteristic equation, it can be shown [1] that the domain of stability can be expressed graphically as in **Figure 2**.

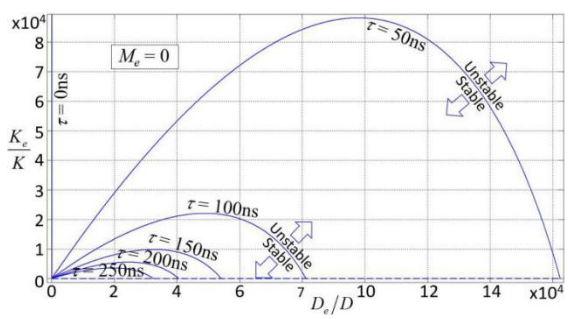

Figure 2: Families of domains of stability for K_e/K versus D_e/D for a variety of feedback delay times. The domains of stability are shown bounded between the horizontal dashed line at $K_e/K=-1$ and the lobes for a given latency τ.

2.2 Equivalent MEMS Circuit

For the MEMS device depicted in **Figure 1**, its equivalent circuit [3][4] is represented in **Figure 2**. The transduction factors are $\eta = 2NCV_0\varepsilon h/g$, where N = number of fingers, ε = permittivity, h = layer thickness, and g = finger gap.

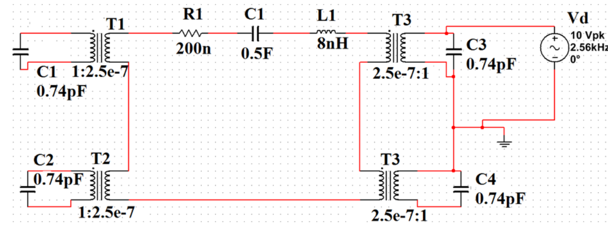

Figure 3: MEMS equivalent circuit. Electrical transducers represent the transformation between the electrical and mechanical domains. Electrical components represent the mechanical components as: $L_1 \rightarrow M$, $R_1 \rightarrow D$, $C_1 \rightarrow 1/K$.

Our testcase (**Fig. 1**) parameters are: $M = 8\text{ng}$, $K = 2\,\text{N/m}$, $D = 2\times10^{-7}\ \text{Ns/m}$, and $N_{in} = N_s = N_f = 140$, $h = 20\mu\text{m}$.

2.3 Feedback Circuit

According to (1), to realize a controllable effective stiffness, damping, and mass, the feedback forces need to be proportional to displacement, velocity, and acceleration. In the feedback circuit, the input is the sensed current i_{sense} from comb senor:

$$i_{sense} = V_{sense}\frac{d}{dt}C_{sense} = V_{sense}\Phi\dot{x} \quad (2)$$

where V_{sense} is the constant voltage applied across the comb sensor and $\Phi = 2N\varepsilon h/g$ is the capacitance per unit deflection. Displacement or acceleration of the proof mass is found by integrating or differentiating i_{sense} respectively as $G_K\int i_{sense}\,dt = G_K\,\Phi V_{sense}\,x$ or $G_M\,di_{sense}/dt = G_M\,\Phi V_{sense}\,\ddot{x}$, where the Gs are tunable gains. Since the comb drive supplies a force that is proportional to the square of the applied voltage, it is necessary to apply the square root of voltage via the feedback loop as $V_K = R_{fb}\sqrt{G_K\Phi V_{sense}\,x}$, $V_D = R_{fb}\sqrt{G_D\Phi V_{sense}\,\dot{x}}$ and $V_M = R_{fb}\sqrt{G_M\Phi V_{sense}\,\ddot{x}}$. Therefore, the feedback forces are

$$\begin{aligned} F_K &= V_K^2 N\varepsilon_0 h/g = \left[G_K R_{fb}^2\,\Phi V_{sense}\,N\varepsilon_0 h/g\right]x = [K_e]x \\ F_D &= V_D^2 N\varepsilon_0 h/g = \left[G_D R_{fb}^2\Phi V_{sense}\,N\varepsilon_0 h/g\right]\dot{x} = [D_e]\dot{x} \\ F_M &= V_M^2 N\varepsilon_0 h/g = \left[G_M R_{fb}^2\,\Phi V_{sense}\,N\varepsilon_0 h/g\right]\ddot{x} = [M_e]\ddot{x}. \end{aligned} \quad (3)$$

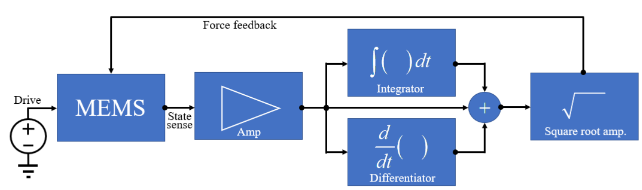

Figure 4: System-level view of the PODMEMS feedback circuit. The circuit-level view within the blocks are given in **Figure 5**. The equivalent circuit of the MEMS bock is given in **Figure 3**.

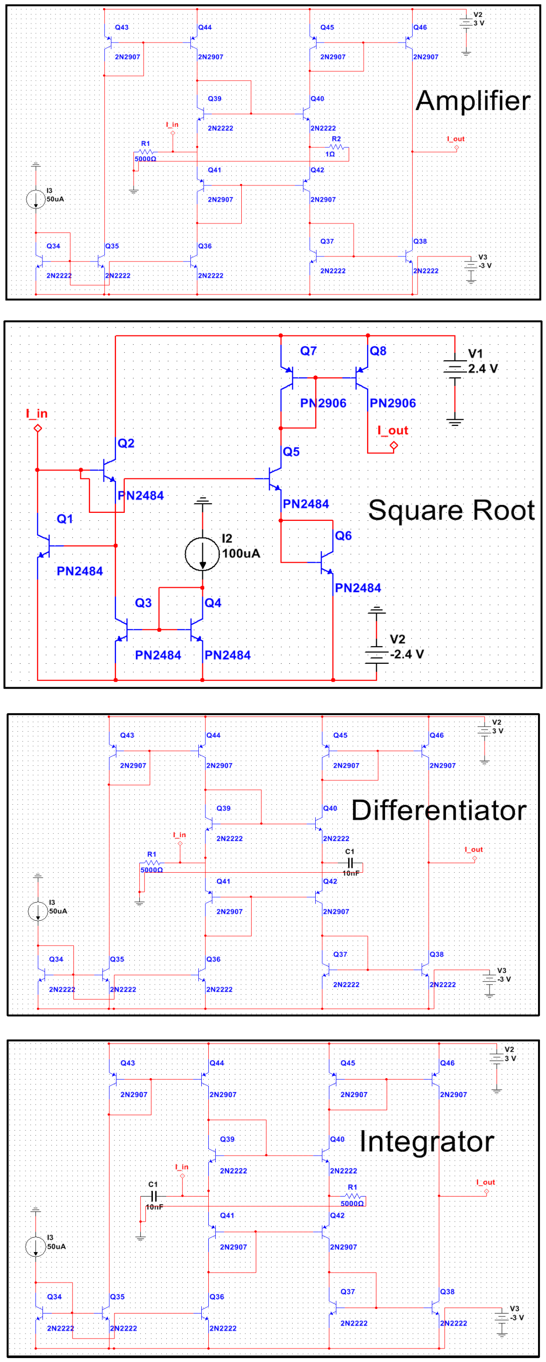

Figure 5: System components of the PODMEMS feedback circuit using BJTs (as modeled in MicroSim[TM]).

A system-level view of PODMEMS components is shown in **Figure 4**. The circuit-level view of each component (integrator, differentiator, square root, and amplifier) is provided in **Figure 5**. The effective mathematical operations of these blocks are:

$$\text{Amplifier block: } i_{amp,out} = \frac{R_1}{R_2} i_{comb\,sensor,in} \tag{4}$$

$$\text{Differentiator block: } i_{differentiator,out} = C_1 R_1 \frac{d}{dt} i_{amp,in} \tag{5}$$

$$\text{Integrator block: } i_{integrator,out} = \frac{1}{C_1 R_1} \int i_{amp,in}\, dt \tag{6}$$

$$\text{Square root: } i_{sqrt,out} = \sqrt{i_{amp,in} + i_{differentiator,in} + i_{integrator,in}}\,. \tag{7}$$

3 RESULTS

In this section we demonstrate performance control over effective stiffness, damping, and mass of our equivalent circuit of PODMEMS by examining the expected results of the frequency response, and we examine the feedback latency by computing signal propagation times.

The frequency of responses of our electrically-modeled system from **Figure 4** is shown in **Figures 6** to **8**, where the family of curves represent the effect that variations in electrical damping, stiffness, and mass have on the behavior of the system. For ease of verification, the response without feedback is given in color blue, and it is the same in all three figures, while changes in effective damping, stiffness, or mass are strategically chosen to halve or double the amplitude and or frequency. The parameters used for our testcase are given in Section 2.2.

It can be shown [6] that an analytical expression that relates the displacement amplitude at resonance to the effective mass, damping, stiffness, and comb drive force amplitude is given by

$$x_{\max} \approx \frac{F_{dr,\max}}{D_{eff}} \sqrt{\frac{M_{eff}}{K_{eff}}}\,. \tag{8}$$

From (8) it is seen that doubling or halving the effective damping will half or double the amplitude, which is verified in **Figure 6**. By quadrupling or quartering the effective stiffness, the amplitude will half or double, and the frequency

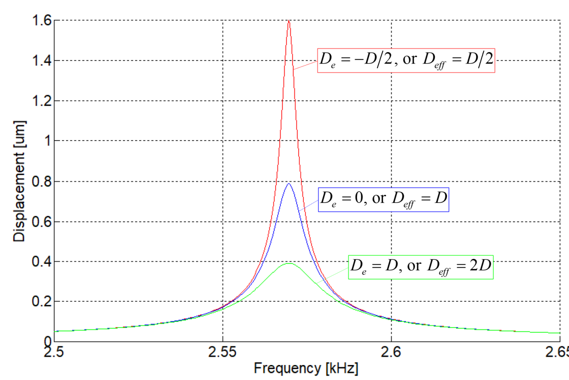

Figure 6: Frequency response of the PODMEMS system from **Figure 4** subject to an electrostatic feedback force that mimics the effect of increased damping (green) or decreased damping (red). The value of D is that of ambient air damping.

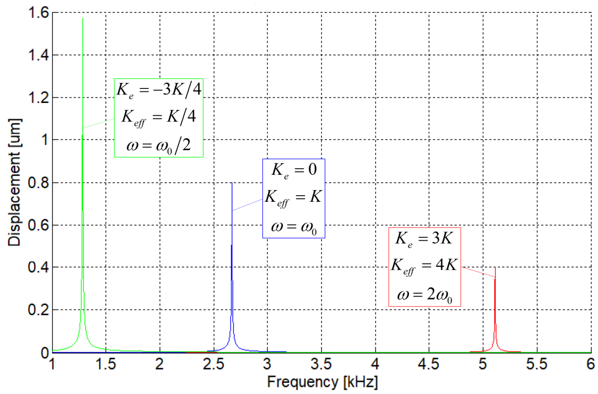

Figure 7: Frequency response of the PODMEMS testcase subject to an electrostatic feedback force that mimics the effect of quadrupling the effective stiffness (red) or quartering the effective stiffness (green).

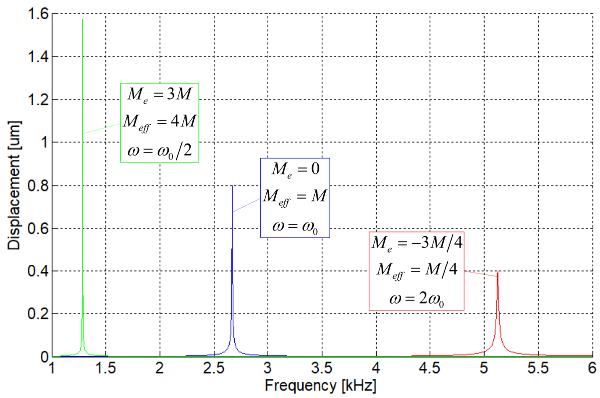

Figure 8: Frequency response of testcase subject to an electrostatic feedback force that mimics the effect of quadrupling the effective mass (green) or quartering the effective mass (red).

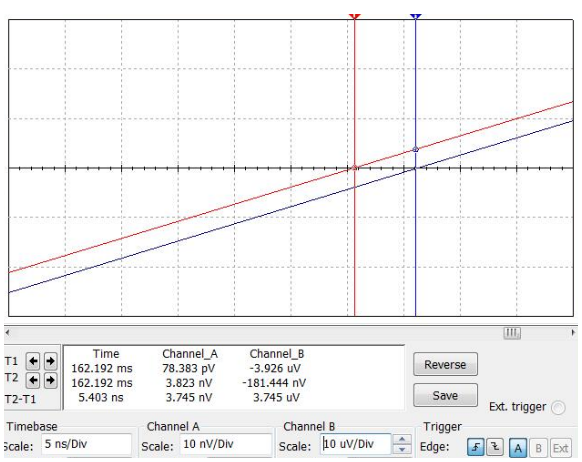

Figure 9: Determination of latency. A sinusoidal input (red) and its output (blue) as processed through our PODMEMS BJT circuit model of **Figures 4** and **5**. The difference between the signals as they cross a horizontal axis is 5.4 nanoseconds.

will double or half, respectively (**Figure 7**). And vice versa for effective mass (**Figure 8**).

Last, we verify that the BJT-based force feedback circuit has a smaller latency than its opamp-based counterpart [1] by comparing the timeline of the processed output signal with the input signal. As verified in **Figure 9**, the BJT-based feedback circuit is about an order of magnitude faster, which greatly enlarges the domain of stability (**Figure 2**).

4 CONCLUSION

In this paper we explored the use of the mathematical functionality of BJT circuit elements to perform proportional gain, addition, differentiation, integration, and square rooting, and do so at a reduced latency when compared to our prior feedback circuit that was based on opamps. We developed an equivalent circuit of our MEMS device so that both the mechanics and electronics could be fully modeled in a common circuit simulator. We found that the BJT-based system was able to reduce the latency by an order of magnitude. That is, the feedback circuit took about 5 nanoseconds to sense the state of the MEMS structure and feedback a proportional force in order to increase or decrease its apparent mass, damping, or stiffness. The decreased latency is beneficial for MEMS structures that resonate at a much faster frequency, as well as for extending the stable and controllable domain of PODMEMS systems.

REFERENCES

[1] J. V. Clark, O. Misiats, S. Sayed, “Electrical control of effective mass, damping, and stiffness of MEMS devices”, *IEEE Sensors Journal*, 2017, Vol. 17, No. 5, pp. 1363-1372.

[2] M. A. Ibrahim, H. Kuntman, and O. Cicekoglu, “A very high-frequency CMOS self-biasing complementary folded cascode differential difference current conveyor with application examples,” *The 2002 45th Midwest Symposium on Circuits and Systems* (*MWSCAS-2002*), Tulsa, OK, USA, 2002.

[3] S. D. Senturia, *Microsystem design*, Springer Science & Business Media, 2007.

[4] H. A. C. Tilmans, “Equivalent circuit representation of electromechanical transducers: I. Lumped-parameter systems”, *Journal of Micromechanics and Microengineering*, 1996, Vol. 6, No. 1, pp. 157-176.

[5] Personal communication with Professor Bogdan Wilamowski of Auburn University, USA, 2017.

[6] G. Fowles, *Analytical Mechanics*, Holt, Rinehart & Winston, 1986.